

## Geochemical assessment of Simav geothermal field, Turkey

**Yildiray Palabiyik and Umran Serpen\***

*Istanbul Technical University, Faculty of Mines, Petroleum and Natural Gas Engineering Department,  
34469 Maslak, Istanbul, Turkey.*

*\* serpen@itu.edu.tr*

### ABSTRACT

*In this study, geochemical methods are used to reliably analyze and understand the Simav geothermal field whose thermal water is rich in terms of Na-HCO<sub>3</sub>-SO<sub>4</sub> and is affected by groundwater which is low in Cl. The water is of meteoric origin and belongs mostly to the immature water group. Quartz and Na-K geothermometers are used to calculate the reservoir temperatures as 70-195 °C and 167-249 °C, respectively, and the Na-K-Mg geothermometer indicated temperatures of approximately 230-240 °C. The isotopic evaluation of the geothermal system indicates that the water in the Simav geothermal reservoir is <sup>18</sup>O enriched, is fed by cold water from Nadarçam and that the age of the water is older than 50 years. The alteration mineralogy of the field points out to reservoir temperatures between 160 °C and 250 °C in the thermal water. The activity diagrams of the thermal water indicate the existence of fluid-rock interaction and show that the water is in equilibrium with K-feldspar, muscovite, albite (Na-feldspar), Mg-chlorite and epidote minerals at a temperature range of 150-250 °C. The activity diagrams also point to a potential source that might be located in a deeper zone that is hotter than the reservoir currently used for production, which is consistent with the alteration mineralogy of the field and Na-K geothermometers. The mineral equilibrium diagrams yield reservoir temperature values that are in harmony with the values obtained from the production zone and silica geothermometers. According to the mineral equilibrium diagrams, it is probable that calcite precipitates at high temperatures and that silica precipitates at low temperatures.*

*Keywords: water chemistry, geothermometry, isotopic evaluation, fluid-rock interaction, fluid geochemistry, Simav geothermal field, Turkey.*

### RESUMEN

*En este trabajo se usan métodos geoquímicos para analizar y entender el campo geotérmico Simav, cuyas aguas geotérmicas son ricas en Na-HCO<sub>3</sub>-SO<sub>4</sub> y son afectadas por aguas subterráneas con bajo contenido de Cl. El agua es de origen meteórico y pertenece principalmente al grupo de aguas inmaduras. Se usaron los geotermómetros de cuarzo y Na-K para calcular las temperaturas del reservorio en 70-195 °C y 167-249 °C, respectivamente, mientras que el geotermómetro de Na-K-Mg indicó temperaturas de aproximadamente 230-240 °C. La evaluación isotópica del sistema geotérmico indica que el agua del reservorio geotérmico de Simav está enriquecida en <sup>18</sup>O, es alimentada por agua fría de Nadarçam y tiene una edad mayor a 50 años. La mineralogía de alteración del campo indica temperaturas entre 160 °C y 250 °C en el agua termal. Los diagramas de actividad de las aguas termales indican la existencia de interacción agua-roca y muestran que el agua está en equilibrio con feldespato potásico, muscovita, albita (feldespato sódico), clorita de Mg y epidota, en un rango de temperatura de 150 a 260 °C. Los diagramas de actividad también señalan una fuente potencial que podría estar localizada en una zona más profunda y más caliente que el reservorio que actualmente está en producción, lo cual es consistente con la mineralogía de alteración del campo y los geotermómetros de Na-K. Los valores de*

temperatura del reservorio derivados de los diagramas de equilibrio mineral concuerdan con los valores obtenidos de la zona de producción y de geotermómetros de sílice. De acuerdo con los diagramas de equilibrio mineral es probable que calcita precipite a altas temperaturas y que sílice precipite a bajas temperaturas.

**Keywords:** *Química de aguas, geotermometría, evaluación isotópica, interacción agua-roca, geoquímica de fluidos, campo geotérmico de Simav, Turquía.*

## INTRODUCTION

The Simav geothermal field, one of Turkey's most important fields, is located in Kütahya's Simav graben system of western Anatolia. Known for the Eynal, Çitgöl and Naşa hot springs, the Simav geothermal field is primarily utilized for balneotherapy and heating for greenhouses and residences. The geothermal fluid produced from the field has been used in a district heating system for the equivalent of 6,000 residences. In the near future, heating for the equivalent of 4,000 residences will be added to that figure. The utilization of the field for power generation is being favorably debated due to the fact that the reservoir temperature exceeds the temperature needed to heat the residences. There are two primary geothermal occurrences in the field: Eynal and Çitgöl-Naşa (Figure 1). Geologic, isotopic and water chemistry data from previous periods are used to generate a general geochemical evaluation that covers the time periods before and after the field began to be used for production, which has been going on since 1993. In addition, various geochemical softwares are used

to interpret and evaluate the fluid-rock interaction as well as the current alteration mineralogy. Investigation is carried out to determine whether the geothermal system has a deeper and hotter component. The geochemical investigation is conducted to determine the origin, residence time and probable route of the geothermal fluid as well as to evaluate the issue of whether the temperature is sufficient to enable power generation from the geothermal system.

The purpose of this study is to use various geological, water chemistry and isotopic data to investigate the characteristic geochemical features of a hydrothermal system and to study the fluid-rock interaction with geochemical models.

## GEOLOGICAL SETTING

The Simav geothermal field is located in the eastern part of Simav graben, approximately 4 km north of Simav town and on the NE edge of the Simav plain, which is separated from the mountain by a high and steep escarpment

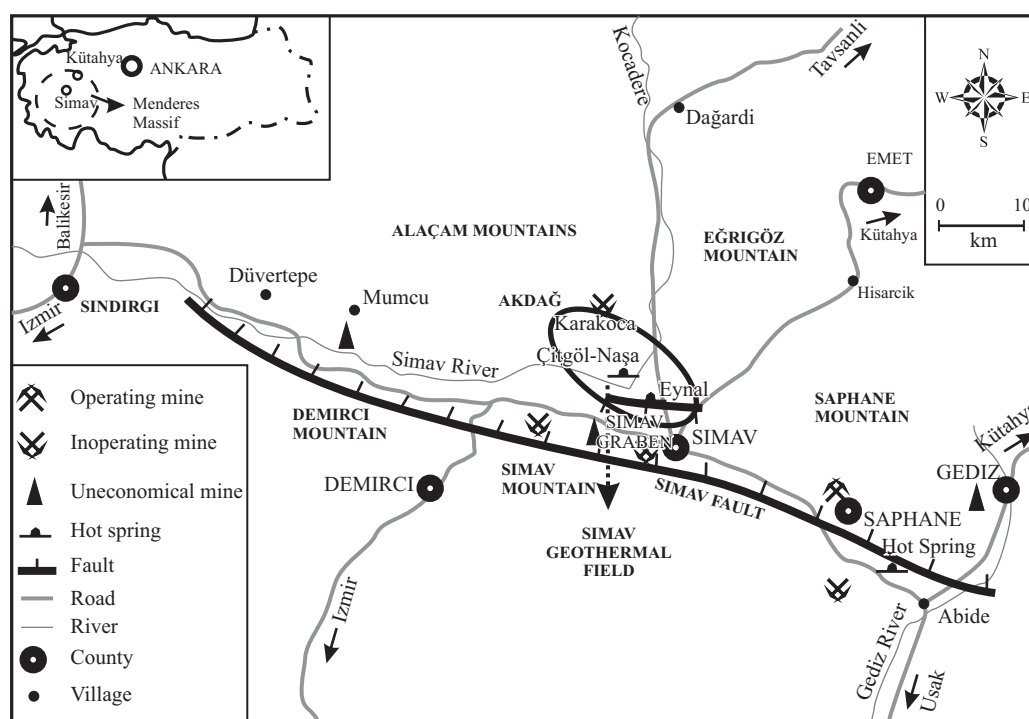


Figure 1. Location map of Kütahya-Simav geothermal field, Turkey (Oygür and Eler, 2000).

(Figures 1 and 2). The plain covers an area of about 70 km<sup>2</sup> and is at an altitude of about 780 m asl. In contrast, Simav Mountain, which is a horst structure located to the south of the plain, reaches an altitude of 1,780 m asl.

**Geology**

The stratigraphic sequence of the formations in the Simav region is given in Figure 2. Paleozoic metamorphic rocks are located at the base of the rock strata in the region. These rocks form the mountains that border the graben on both sides, and outcrop frequently in these mountains. Also, it is known that under the graben these rock units are underlain by younger sedimentary rocks. The metamorphic rocks are covered by a layer of lower Mesozoic rocks and Jurassic carbonates that have not been metamorphosed, which also

overlay the metamorphites in the Simav horst to the south of the graben as well as in the relatively lower Akdağ horst to the north. These rocks are overlain by volcanic rocks and lake sediments of Miocene age that were deposited in the graben along a NNE-SSW axis or formed in relation to those grabens. These formations appear on the Simav horst to the south of the graben as well as on ridges of the arm to the north of the graben, which has risen to a lower altitude. These are followed by younger formations which precipitated or formed together with the Simav graben or at a later time (Akdeniz and Konak, 1979). These are spread out over the graben interior areas, which have been downthrown significantly compared with the horsts on both sides of the Simav graben. The coarse-grained terrestrial sediments, basaltic lava deposits and thick alluvium have created a layer in the graben that is hundreds of meters thick (Öngür, 2004). Based on the existing wells drilled in the region, the

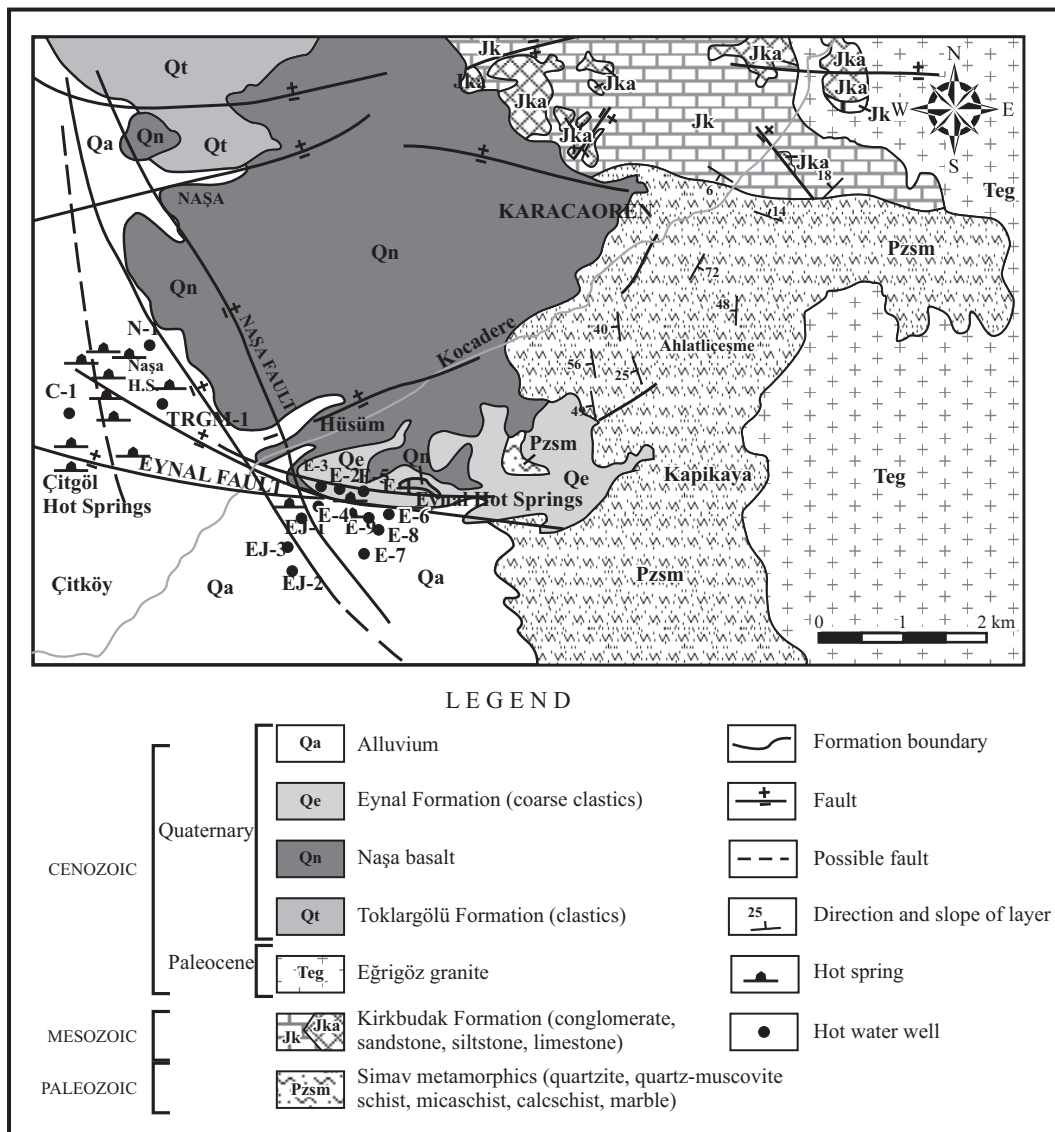


Figure 2. Geological map of Kütahya-Simav geothermal field (Akkus *et al.*, 2005).

fractured reservoir rocks producing hot fluids in the field largely consist of Naşa Basalt, Simav metamorphics and Mesozoic limestones, while the cap rock consists of Tertiary strata of volcano-sedimentary rock.

Western Turkey and the southern Basin and Range, USA, are two of the best examples of large continental extension and exhibit remarkable similarities and some unique differences. The two regions contain structural features unique to extension such as metamorphic core complexes, extensional folds, shear zones, and detachment surfaces, although the origin of extension is different (Cemen *et al.*, 2002). In extensional tectonic regimes like the Basin and Range province and the Anatolia Belt of western Turkey, extensional detachments have created favorable structures for geothermal occurrences.

Three crustal segments, namely central core, southern and northern submassifs, differing in structure and cooling history have been identified in Menderes Massif of western Turkey by Ring *et al.* (2003). The Simav detachment, formed later, reactivated the Eocene Cyclades-Menderes thrust and its initial movement was synchronous with the intrusion of Eğrigöz granites (Ring *et al.*, 2003).

After Miocene, western Anatolia has undergone the extensional regime that helped build the actual form. This process produced the Simav graben, which has an asymmetric structure. The southern part of the graben is limited by the Simav fault, which is roughly extended in west-east direction for more than 80 km and separates Simav Mountain from Simav plain. In addition to the Simav geothermal system, there are geothermal occurrences at both extremes of the Simav fault (Düvertepe and Saphane). Extending in a corridor-like narrow structure, the Simav fault is expanded around the Simav plain gaining the features of a typical graben-like structure with a triangular shape that resembles a pull-apart type basin, which is delimited by a few extensional faults (Eynal, Naşa) in the northern section.

The Simav fault with a slip of 1,000 m is located at the southern flank of Simav graben and formed at a later phase, probably during Pliocene, together with major grabens within the Menderes massif. Although the Eynal, Çitgöl and Naşa hot springs discharge at the northern flank of the Simav graben along the Eynal and Naşa faults, deep conductive anomalies identified by geophysical studies are located at southern flank close to the Simav fault. These deep conductive anomalies are also related to shallower conductive anomalies found close to Eynal and Naşa faults. Therefore, it is believed that the deeply slipped Simav fault plays a primordial role in the formation of the Simav geothermal system.

### Heat source

Hochstein *et al.* (1990) and Zhongke *et al.* (1990) described and studied low temperature fracture-zone systems in SE Asia. Turkey is also known to have many low

to moderate temperature geothermal resources (Serpen and Mihcakan, 1999) and most of these resources are related to important fracture systems. The major geothermal systems of western Turkey are all structurally similar geothermal occurrences. A conceptual hydrological model may be hypothesized to explain the likely heat and mass transfer of the Simav geothermal system. The Simav fault penetrates very deep to communicate a deep heat sweep of naturally convecting meteoric waters in the metamorphic crust. Hochstein *et al.* (1990) pointed out that fracture zone systems, which are driven by higher than normal heat flow, occur in areas underlain by thinner continental type of crust (*i.e.*, systems in the Basin and Range tectonic province of USA or Menderes massif of Turkey). An earlier theoretical study by Kassoy and Zebib (1978) also showed that fluid convection can occur in a narrow fracture zone which stands in a crustal environment with normal temperature. The Simav geothermal system is thought to be controlled by the active Simav fault and probably driven by higher than normal heat flow, 110 mW/m<sup>2</sup> (Ilkisik, 1995), in the Aegean region of Turkey, and terrain-induced forced convection. With prevailing temperatures of 160 °C at economic depths (less than 1 km) within the fracture zone reservoir, the Simav geothermal system resembles “the fracture zone systems with high temperatures at sweep base” described by Hochstein (1990).

### Alteration mineralogy

Unfortunately, we do not have access to any core sample or cuttings from drillings that have been taken from wells in the Simav geothermal field. But surface geological studies indicate alteration minerals alunite (Burcak *et al.*, 2007) and kaolinite along the Simav fault (from Düvertepe to Saphane). Although the alteration mineralogy of the Simav geothermal field is not well known, the mineralogical data from 14 rock samples were presented in a study by Öktü (1984). The rock samples that have been taken from Simav, Kütahya and the surrounding areas were used for an evaluation of the alteration mineralogy in this study. In the light of these mineralogical data, the primary alteration minerals observed in the Simav geothermal field include chlorite, albite, K-feldspar, epidote, muscovite, illite, and montmorillonite. Of these minerals, the ones that are most notable with regard to hydrothermal alteration are chlorite, K-feldspar, illite, montmorillonite and epidote. This is because epidote (Ca[Al,Fe]<sub>3</sub>Si<sub>3</sub>O<sub>12</sub>OH) generally occurs in geothermal fields with temperatures between 200 and 250 °C (Bird *et al.*, 1984). On the other hand, illite is a clay mineral that is identified with X-ray diffraction data and is generally observed in fields with temperatures over 180 °C (Browne, 1996). From this information, it can be concluded that the Simav geothermal field is a high-temperature one, with alteration mineralogy that should be carefully studied in future.

## HOT SPRINGS AND WELLS

There are hot water springs in the region that existed before the wells were drilled, although some of these springs still appear during the summer. According to Yücel *et al.* (1983), there are four large hot springs that outflow from alluvium and debris from slopes in the Eynal area and ten large springs that outflow from the alluvium in the Çitgöl-Naşa area. Öktü (1984) reported that there were a total of 89 hot water springs in the region, consisting of 34 in the Eynal area and 55 in the Çitgöl-Naşa area. Springs in the Eynal area are generally hotter than those in the Çitgöl-Naşa area and outflow in a E-W linear fashion along faults, with flow rates that vary between 0.02 L/s and 0.2 L/s, with a total flow of 2.1 L/s and temperatures that vary between 51 °C and 96 °C. The flow rates of springs in the Çitgöl-Naşa area vary between 0.15 L/s and 0.86 L/s, while temperatures vary between 34 °C and 86 °C.

Drilling in the region was started in 1985 by the General Directorate of Mineral Research and Exploration in Turkey (MTA). Currently there are a total of 11 exploration and production wells that are active in the region, including five in the Eynal hot springs area (E-1, E-2, E-3, E-7 and E-8) and three in the Çitgöl-Naşa hot springs area (C-1, C-2 and N-1). Later, three deeper exploration and production wells (EJ-1, EJ-2 and EJ-3) were drilled to the south of Eynal in conjunction with the Simav District Heating Project. The depth of the wells in the Simav field varies between 65.8 m (E-1) and 958 m (EJ-2) while the bottom-hole temperatures varied between 105 °C (C-1) and 162 °C (EJ-1). Information regarding the depth, level of production, temperature, production flow rate, reservoir rock type and date of drilling for certain wells in the region are shown in Table 1.

## WATER CHEMISTRY

In the regional framework, the majority of west Anatolian geothermal waters are either Na-HCO<sub>3</sub> or Na-Cl in nature, although SO<sub>4</sub>-type waters are also present. The waters are weakly acidic to alkaline with pH values ranging from 6.1 to 9.6, and have total dissolved solids (TDS) contents between 550 and 54,884 ppm (Mutlu and Gulec, 1998).

Chemical compositions of waters from thermal springs and wells from Eynal and Çitgöl-Naşa areas of Simav region are summarized in Table 2. The pH of most of the waters in the study area is between 7 and 9 giving them a slightly alkaline character that is close to neutral. The concentration of total dissolved solids in water vary between 1,400 and 3,000 mg/L. The waters from the Simav region can be classified as Na<sup>+</sup>>K<sup>+</sup>>Ca<sup>+</sup> according to dominant cations and as HCO<sub>3</sub><sup>-</sup>>SO<sub>4</sub><sup>2-</sup>>Cl<sup>-</sup> according to dominant anions. With HCO<sub>3</sub><sup>-</sup> as the dominant anion and Na<sup>+</sup> as the dominant cation, these waters are also classified as soda waters. Similar types of waters seem to occur in different parts of the Simav region. As is true with thermal springs like Gediz-Abide and Saphane in the surrounding regions, waters in Simav region are high in SO<sub>4</sub><sup>2-</sup> and F<sup>-</sup>, and low in Cl<sup>-</sup> (Burcak *et al.*, 2007). The primary source of high sulfate concentrations in waters is thought to be alunite that has formed from the alteration of tuffs that outcrop over a large area around Saphane, which is situated about 20 km east of Simav. It is very likely that thermal water in this region leaches sulfate from these rocks. On the other hand, the source of high F concentration in waters is probably the fluorite in the alteration zones of migmatitic and granitic rocks.

Thermal and cold springs in the Simav region are compositionally different. Underground waters in the region

Table 1. Data relevant to the Simav geothermal wells.

Well <sup>a</sup>	Latitude	Longitude	Depth (m)	Production level (m)	Reservoir rock	Depth interval of reservoir rock (m)	Well head temperature (°C)	Bottom hole temperature (°C)	Flow rate (L/s)	Date
E-1	33069.3	72313.5	65.8	–	Naşa Basalt	50 – 65.8	97	143	14	1985
E-2	33049.6	72208.4	149.5	120	Simav Metamorphics	84 – 149.5	97	158	55	24.07.1985
E-3	33100.9	72071.4	150	120	Simav Metamorphics	92 – 150	97	149	50	25.09.1985
E-4	33060	71985	220	–	Simav Metamorphics	–	98	–	1	1994
E-5	33062.6	72278.1	300	–	Simav Metamorphics	74 – 300	97	–	6	24.10.1994
E-6	32862.7	72688.53	169.6	–	Simav Metamorphics	135 – 169.6	–	157	50	25.12.1994
E-7	32687	72527	475	63	Alluvium	3 – 97	52	–	0.25	06.01.1997
E-8	32836	72638	205	–	Simav Metamorphics	180 – 205	–	161	60–80	08.03.1997
EJ-1	32708.84	71952.69	725.2	600	Simav Metamorphics	437 – 650	–	162	72	28.09.1987
EJ-2	32251.2	71732.2	958	462	Simav Metamorphics	457 – 791	–	157	1	02.10.1988
EJ-3	32283	71662	424	–	Budagan Limestone	403 – 424	–	151	40–60	13.04.1997
C-1	33623.3	70029.2	101	46 85	Alluvium Naşa Basalt	0 – 83 83 – 101	97	105	32	14.08.1985
C-2	33570	69900	–	–	–	–	–	–	–	–
N-1	34761.9	69459	200	–	Simav Metamorphics	157 – 200	42	–	2	18.10.1985
N-2	34780	69360	–	–	–	–	–	–	–	–

<sup>a</sup>Yurtseven *et al.* (1998)

Table 2. Data of chemical analyses (ppm) for Simav thermal waters.

Region	Sample	Sampling date	T (°C)	pH	K	Na	Ca	Mg	B <sub>T</sub>	Li	SiO <sub>2</sub>	HCO <sub>3</sub> <sup>-</sup>	SO <sub>4</sub> <sup>2-</sup>	Cl <sup>-</sup>	F <sup>-</sup>	Fe <sub>T</sub>	As <sub>T</sub>	NH <sub>4</sub>	CO <sub>2</sub>	C.B.(%)	Reference	
Eynal	Ey	1983	60	8.2	54	490	5.5	1.3	5.2	0.8	165	518	454	70	18	-	0.2	0.1	5.2	5.28		
	Ey-2	1983	74	8.9	65	530	4.3	1	-	-	190	458	436	69	14	0.1	0.24	0.1	-	12.97		
	Ey-3	1983	63	9.3	59	480	2.9	1	4.5	0.8	165	408	494	71	18	0.1	0.9	0.1	0.8	6.58	a	
	Ey-4	1983	96	9.5	61	600	2	1	5.4	1	218	425	483	73	18	-	1.02	0.1	-	16.57		
	Ey-6	1983	60	8.2	54	490	5.5	1.3	5.2	0.8	165	518	454	70	18	-	0.2	0.1	5.2	5.28		
	E-1 <sup>+</sup>	1985	97	-	48	458	6	-	4.5	-	200	326	417	69	-	-	-	-	-	14.64		
	E-2 <sup>+</sup>	26.11.1985	97	8.7	51	470	6	-	4.3	0.4	50	628	416	72	12	-	0.32	0.66	-	1.11	e	
	E-3 <sup>+</sup>	26.11.1985	97	7.6	48	500	20	3.4	5.9	0.4	46	860	433	76	13	-	0.2	1.24	-	3.24		
	Çiğözü-Naşa	ÇT-1	1983	77	7.2	37	245	43	3.7	2.5	-	165	494	259	30	4.2	-	0.2	0.1	49	1.76	
		ÇT-2	1983	79	7.9	44	355	33	1.8	3.4	-	177	555	340	55	7.7	-	0.02	0.1	11	0.63	
ÇT-3		1983	83	7	44	340	34	5.3	4.2	-	181	573	376	57	7	-	0.09	0.1	92	3.09	a	
ÇT-5		1983	35	8.2	44	350	82	14	3.5	0.8	44	580	317	50	2.9	-	0.1	0.1	58	10.25		
Nş-1		1983	64	6.6	42	395	39	9.6	3.4	0.8	162	604	344	52	5.9	-	0.24	0.1	241	5.67		
Ç-1 <sup>+</sup>		26.11.1985	97	7.2	35	315	49	2.7	3.9	0.2	56	610	300	52	8	-	0.28	0.9	-	2.37	e	
N-1 <sup>+</sup>		26.11.1985	42	7.6	7	126	56	13	2	-	28	500	82	15	1.1	-	0.06	1.8	-	4.33	g	
SE-1		1984	86	7.8	38	440	15	0.2	3.8	-	183	671	382	67	13.8	-	0.42	0.72	-	1.63		
SE-4		1984	53	8.9	47	550	9.1	-	4.3	-	-	500	445	76	15.3	-	0.5	-	-	11.24		
SE-7		1984	51	7.8	30	290	50	10	2.7	-	128	574	238	58	6.5	-	0.26	-	-	1.08		
SE-14	1984	77	8.8	50	530	1.8	-	4.8	-	123	616	453	76	15.3	-	0.51	0.36	-	4.14			
SE-16	1984	68	8.2	50	550	3.8	0.3	5	-	123	629	486	85	18	-	0.46	0.93	-	3.34			
SE-21	1984	51	6.6	13	180	9.6	0.8	1.1	-	183	79	264	18	13	0.64	0.34	5.66	-	4.34			
SE-27	1984	85	8.5	29	480	3.3	-	4.5	-	115	641	445	79	15.8	-	0.52	-	-	2.35			
SE-29	1984	73	8.8	49	540	2.9	-	4.6	-	123	574	467	158	17	-	0.49	0.46	-	0.82			
SE-36	1984	64	8.1	43	400	17	0.4	3.8	-	175	685	364	61	12.8	-	0.24	-	-	4.49			
SE-41	1984	82	9.6	35	410	4	-	4.6	-	190	470	427	79	18	-	0.51	0.36	-	2.17			
SE-43	1984	52	7.1	41	410	8.7	0.1	4.4	-	175	549	422	70	15.5	0.2	0.52	-	-	3.13			
SE-47	1984	70	7.8	42	450	17	0.3	4.7	-	150	647	426	76	14.5	-	0.55	-	-	1.96			
SE-48	1984	62	9.8	44	430	5.4	0.2	3.9	-	195	641	366	67	13	-	0.45	0.15	-	1.44			
SE-52	1984	62	7.4	25	460	2.8	-	4.5	-	143	582	423	75	15.8	0.24	0.54	0.36	-	1.20	b		
Çiğözü-Naşa	ŞÇN-1	1984	34	7.9	7	45	69	20	0.3	-	68	372	27	12	0.46	-	0.09	-	-	1.42		
	ŞÇN-2	1984	67	8.2	30	300	59	13	3.1	-	183	622	306	58	5	-	0.49	1.7	-	1.75		
	ŞÇN-4	1984	38	8.3	37	360	50	9	3.1	-	148	616	309	109	6.8	-	0.36	-	-	0.31		
	ŞÇN-11	1984	61	7.4	38	320	53	9	3.2	-	148	641	294	52	6.8	-	0.32	-	-	0.48		
	ŞÇN-13	1984	59	8.2	31	225	72	16	1.9	-	148	525	280	49	5	-	0.16	-	-	1.88		
	ŞÇN-17	1984	60	8.1	36	220	61	11	2	-	115	494	291	21	6	-	0.17	0.93	-	2.12		
	ŞÇN-21	1984	75	8.5	35	338	30	3.6	3	-	138	360	390	79	8.5	-	0.27	0.98	-	2.04		
	ŞÇN-23	1984	55	7.5	47	390	35	7	4	-	140	622	397	61	8	-	0.31	-	-	0.28		
	ŞÇN-25	1984	55	7.6	43	460	34	6.3	3.6	-	190	744	404	67	8.5	-	0.37	-	-	0.82		
	ŞÇN-30	1984	86	7.3	38	360	37	3.9	3.3	-	195	580	366	61	7.3	-	0.45	0.93	-	1.14		
ŞÇN-32	1984	77	7.1	27	240	44	4.1	2.4	-	140	488	220	41	4.4	-	0.26	0.36	-	1.11			
ŞÇN-33	1984	39	7.1	30	275	79	9.2	3.1	-	140	592	288	55	3.5	-	0.22	0.93	-	0.02			

Table 2. (Cont.) Data of chemical analyses (ppm) for Simav thermal waters.

Region	Sample	Sampling Date	T (°C)	pH	K	Na	Ca	Mg	B <sub>T</sub>	Li	SiO <sub>2</sub>	HCO <sub>3</sub> <sup>-</sup>	SO <sub>4</sub> <sup>2-</sup>	Cl <sup>-</sup>	F <sup>-</sup>	Fe <sub>T</sub>	As <sub>T</sub>	NH <sub>4</sub>	CO <sub>2</sub>	C.B.(%)	Reference
Eynal	EY-1	1995	79	8.2	55	300	60	10	-	-	-	1166	314	80	-	0.02	-	-	-	-	20.87
	EY-2	1995	80	8.7	45	460	40	10	-	-	-	602	319	82	-	0.45	-	-	-	-	12.04
	EY-3	1995	67	8.8	75	450	25	10	-	-	-	499	309	83	-	0.15	-	-	-	-	16.31
Çitgöl-Naşa	NAŞA-1	1995	65	6.6	30	303	70	15	-	-	-	567	254	60	-	0.21	-	-	-	-	6.86
	NAŞA-2	1995	45	6.8	30	363	80	15	-	-	-	783	256	66	-	0.05	-	-	-	-	4.20
	ÇITGÖL-2	1995	88	9.1	35	360	35	5	-	-	-	403	285	69	-	0.08	-	-	-	-	12.73
	Nadarcam <sup>a</sup>	1995	12	7.3	9	4.4	68	31	-	-	-	283	27.7	8.9	-	-	-	-	-	-	7.59
Eynal	EY-1	1996	79	8.2	58	300	58	10	-	-	-	556	351	59	-	15.03	-	-	-	-	0.45
	EY-2	1996	64	8.5	43	380	25	7.5	-	-	-	552	378	64	-	0.17	-	-	-	-	2.01
	EY-3	1996	87	7.4	5	2.3	39	2	-	-	-	126	7.5	2	-	4.97	-	-	-	-	1.31
Çitgöl-Naşa	NAŞA-1	1996	57	6.1	35	325	60	10	-	-	-	604	325	55	-	0.28	-	-	-	-	1.70
	NAŞA-2	1996	50	6.6	45	306	73	12.5	-	-	-	670	310	55	-	0.37	-	-	-	-	0.38
	ÇITGÖL-2	1996	89	9.7	43	342	30	5	-	-	-	421	352	63	-	3.2	-	-	-	-	5.54
Eynal	EY-1	1997	81	7.5	40	510	53	5	-	-	69	745	449	82	-	-	-	-	-	-	4.77
	EYNAL	1997	96	8.3	40	520	65	7.5	-	-	54	592	530	78	-	-	-	-	-	-	9.05
	EY-5	1997	90	8.8	55	535	128	7.5	-	-	120	446	610	89	-	-	-	-	-	-	16.90
Çitgöl-Naşa	ÇITGÖL-2	1997	70	7.9	20	278	54	7	-	-	63	416	324	53	-	-	-	-	-	-	2.63
	NAŞA-1	1997	51	6.1	25	335	88	9	-	-	41	680	346	57	-	-	-	-	-	-	0.95
Eynal	EY-Ç	22.09.1948	78	7.8	53	482	8	6.8	-	-	60	769	420	71	-	0.12	-	0.15	-	-	0.16
	EY-G	22.09.1948	68	7.3	46	376	31	24.8	-	-	63	706	362	64	-	0.12	-	0.15	53	-	0.48
	EY-E	22.09.1948	66	7.4	46	374	38	15.5	-	-	68	659	382	68	-	0.024	-	-	31	-	0.14
	EY-K	22.08.1948	68	7.4	47	396	20	7.4	-	-	40	667	349	58	-	0.082	-	0.3	22	-	0.50
Çitgöl-Naşa	NŞ-Ç	22.09.1948	52	7.1	37	282	56	8.5	-	-	34	615	278	46	-	0.182	-	1.75	114	-	1.36
	NŞ-N	22.09.1948	43	7.2	34	275	57	17.1	-	-	52	583	303	48	-	0.184	-	0.2	97	-	0.40
Eynal	EI-1 <sup>+</sup>	1987	162 <sup>*</sup>	9.2	57	530	16	4.8	8.4	2.6	115	244	471	85	13	-	-	1.8	50	-	21.39
	E-7 <sup>+</sup>	11.01.1997	52	7.4	28.8	397	32	9.73	2.64	-	234	805	315	46	5.9	-	-	1.39	-	-	2.30
	E-8 <sup>+</sup>	05.05.1997	161 <sup>*</sup>	8.2	61.2	409	33	1	6.2	2.6	165	976	758	86	14	0.3	-	0.6	-	-	23.91
	EI-3 <sup>+</sup>	05.05.1997	151 <sup>*</sup>	8.2	39.3	400	5.6	2.14	6.4	2.8	165	854	533	82	9.3	0.1	-	0.6	-	-	18.31

<sup>a</sup>Yücel *et al.* (1983), <sup>b</sup>Öktü (1984), <sup>c</sup>Bayram and Simsek (2005), <sup>d</sup>Çaglar (1948), <sup>e</sup>Erişen *et al.* (1989), <sup>f</sup>Yurtseven *et al.* (1998), <sup>g</sup>Güven and Taskin (1985), <sup>h</sup>Cold spring, <sup>i</sup>Well, <sup>j</sup>Bottom-hole temperature, C.B.: Charge-balance of the water.

are rich in  $\text{Ca}^+$  with variable  $\text{Mg}^{2+}$  levels and generally low in alkali contents. Thus, Simav cold springs can be classified as  $\text{CaMg}(\text{HCO}_3)$  waters. Chemistry of hot springs of the Simav region varies with distance from the Eynal fault. While concentrations of  $\text{Ca}^+$  and  $\text{Mg}^{2+}$  of hot springs and wells increase,  $\text{Na}^+$ ,  $\text{K}^+$  and  $\text{SO}_4^{2-}$  concentrations decrease toward Çitgöl and Naşa areas. Since the chemical compositions of thermal springs and wells in the Eynal area are close to each other, a deep rising fluid component through the Eynal fault seems to be important in this area.

Instead of using ternary diagrams to describe trends for data, a simple approach is preferred to investigate bivariate correlations for some chemical parameters utilized in ternary diagrams using conventional x-y regression analysis. Computer program OYNYL by Verma *et al.* (2006) was used for this purpose. This computer program has the unique feature of a built-in algorithm for discordant outliers detection following the methodology of Barnett and Lewis (1994). Table 3 presents the results of regression analysis for selected chemical parameters in fluids from the Simav geothermal field. As seen in Table 3, of ten pairs of data investigated, a statistically valid correlation at 99% confidence level is obtained for seven pairs:  $\text{SO}_4$ -Cl, Ca-Mg, Na+K-Ca, Na+K-Mg, Cl-B,  $\text{HCO}_3$ -B, and  $\text{HCO}_3$ -Cl. Of these statistically valid correlations, the highest correlation coefficients (around 0.81) are obtained for the pairs  $\text{SO}_4$ -Cl and Ca-Mg. Strong association of Ca-Mg may be attributed to the dissolution of carbonate rocks of Mesozoic and Paleozoic age. Marbles of metamorphic origin in the Menderes massif are known to contain abundant dolomite; therefore, their association might be expected. On the other hand, inverse relation

in Na+K-Ca and Na+K-Mg pairs might be attributed to the enrichment of Na+K and depletion of Ca+Mg as a result of interaction of  $\text{CO}_2$  with water and rocks (Fara *et al.*, 1999). As for the association of Cl-B, they originate from deep waters circulating through Paleozoic age metamorphites.

## GEOOTHERMOMETERS

The computer program SolGeo (Verma *et al.*, in press) was used for processing water chemistry data for solute geothermometry. From the Excel output file of this program, the most important results were extracted and are discussed below.

### Silica geothermometers

The silica geothermometers used on the Simav thermal water samples are presented in Table 4. The silica concentrations for some well samples (E-2, E-3, C-1, N-1) taken in 1985 were very low (28–56 ppm), probably as result of sampling errors or precipitation, and were thus not included in this evaluation. Of the silica geothermometers, Fournier's (1977) quartz-maximum evaporation (88–177 °C), Fournier and Potter's (1982) quartz-adiabatic cooling (86–179 °C), and Arnorsson's (2000) quartz (70–184 °C) geothermometers yielded a temperature range of 70–184 °C, indicating temperatures that are likely to be close to actual reservoir and bottom-hole temperatures, particularly on deep wells in the field. On the other hand,

Table 3. Regression coefficients (ordinary linear correlation) for selected chemical parameters in fluids from the Simav geothermal field using the OYNYL computer program (Verma *et al.*, 2006).

X	Y	n	a	sa	b	sb	r	$P_c(r;n)$	$P_l(r;n)$	CL(%)
$\text{HCO}_3^-$	$\text{SO}_4^{2-}$	68	240	50	0.21	0.08	0.3033	0.0119	0.9881	98.81
$\text{HCO}_3^-$	Cl	68	39	9	0.043	0.015	0.3256	0.0067	0.9933	99.33
$\text{HCO}_3^-$	Cl	67*	37	8	0.043	0.013	0.3822	0.0014	0.9986	99.86**
$\text{SO}_4^{2-}$	Cl	68	15	6	0.136	0.017	0.7009	8.7E-8	>0.99999	>99.999
$\text{SO}_4^{2-}$	Cl	66*	14.9	4.4	0.129	0.012	0.8120	3.2E-8	>0.99999	>99.999**
Na+K	Ca	68	78	10	-0.100	0.023	-0.4740	4.4E-5	0.99996	99.996
Na+K	Ca	67	84	8	-0.118	0.019	-0.6655	5.7E-8	>0.99999	>99.999**
Na+K	Mg	68	14.9	2.1	-0.020	0.005	-0.4595	8.1E-5	0.99992	99.992**
Ca	Mg	68	1.2	0.9	0.143	0.019	0.6786	8.7E-8	>0.99999	>99.999
Ca	Mg	66*	0.1	0.7	0.172	0.016	0.8105	3.2E-8	>0.99999	>99.999**
$\text{SiO}_2$	$\text{HCO}_3^-$	55	630	50	-0.38	0.36	-0.1406	0.3060	0.6940	69.40
$\text{SiO}_2$	$\text{SO}_4^{2-}$	55	320	38	0.45	0.27	0.2192	0.1098	0.8902	89.02
Cl	B	44	1.4	0.5	0.038	0.007	0.6543	1.5E-6	>0.99999	>99.999**
$\text{HCO}_3^-$	B	44	2.5	0.8	0.0025	0.0014	0.2682	0.0784	0.9216	92.16
$\text{HCO}_3^-$	B	43*	1.3	0.7	0.0043	0.0012	0.5049	5.5E-4	0.9994	99.94**

X and Y are regression variables, n: the number of data, a: the intercept of the linear regression, sa: the error of the intercept, b: the slope of the linear regression, sb: the error of the slope, r: the linear regression coefficient,  $P_c(r;n)$ : the probability of no-correlation (Bevington and Robinson, 2003),  $P_l(r;n)$ : the probability of linear correlation, CL: the confidence level. \*: one or more discordant outliers were detected by applying the Barnett and Lewis (1994) methodology programmed in OYNYL (Verma *et al.*, 2006); also includes the application of some tests summarized by Verma and Quiroz-Ruiz (2006a, 2006b). \*\*: statistically valid linear correlations at 99% confidence level.

Table 4. Discharge temperature and temperatures (°C) obtained for Simav thermal waters with the silica (quartz) geothermometers.

Region	Sample	Discharge T (°C)	Quartz <sup>a</sup>	Quartz, maximum evaporation <sup>a</sup>	Quartz <sup>b</sup>	Quartz, adiabatic cooling <sup>b</sup>	Quartz <sup>c</sup>	Quartz, adiabatic cooling <sup>c</sup>	Quartz <sup>d</sup>	Quartz <sup>e</sup>
Eynal	Ey	60	167	158	168	160	158	149	167	168
	Ey-2	74	177	165	177	167	168	158	177	179
	Ey-3	63	167	158	168	160	158	149	167	168
	Ey-4	96	186	173	187	175	178	166	186	189
	Ey-6	60	167	158	168	160	158	149	167	168
	E-1 <sup>+</sup>	97	180	168	181	170	172	161	180	183
	E-2 <sup>+</sup>	97	102	103	102	102	88	89	102	96
Çitgöl-Naşa	E-3 <sup>+</sup>	97	98	99	98	99	84	85	99	92
	ÇT-1	77	167	158	168	160	158	149	167	168
	ÇT-2	79	172	161	172	163	163	153	172	174
	ÇT-3	83	173	163	174	165	164	155	174	175
	ÇT-5	35	96	98	96	97	82	83	97	90
	Nş-1	64	166	157	166	159	157	148	166	167
	Ç-1 <sup>+</sup>	97	107	107	108	107	94	94	108	102
Eynal	N-1 <sup>+</sup>	42	77	81	77	78	62	64	77	69
	SE-1	86	174	163	175	165	165	155	174	176
	SE-7	51	152	145	152	146	141	135	152	151
	SE-14	77	149	143	149	144	138	133	149	148
	SE-16	68	149	143	149	144	138	133	149	148
	SE-21	51	174	163	175	165	165	155	174	176
	SE-27	85	145	139	145	141	134	129	145	144
	SE-29	73	149	143	149	144	138	133	149	148
	SE-36	64	171	161	172	163	162	153	171	173
	SE-41	82	177	165	177	167	168	158	177	179
	SE-43	52	171	161	172	163	162	153	171	173
	SE-47	70	161	153	162	155	151	144	161	162
	SE-48	62	178	167	179	169	170	159	179	181
	SE-52	62	158	150	159	152	148	141	158	158
	SÇN-1	34	117	115	117	116	104	103	117	113
	SÇN-2	67	174	163	175	165	165	155	174	176
	SÇN-4	38	160	152	161	154	150	143	160	161
SÇN-11	61	160	152	161	154	150	143	160	161	
SÇN-13	59	160	152	161	154	150	143	160	161	
SÇN-17	60	145	139	145	141	134	129	145	144	
Çitgöl-Naşa	SÇN-21	75	156	148	156	150	146	139	156	156
	SÇN-23	55	157	149	157	151	146	140	157	157
	SÇN-25	55	177	165	177	167	168	158	177	179
	SÇN-30	86	178	167	179	169	170	159	179	181
	SÇN-32	77	157	149	157	151	147	140	157	157
	SÇN-33	39	157	149	157	151	147	140	157	157
	EY-1	81	117	116	118	117	104	104	118	113
Eynal	EYNAL	96	105	106	106	106	92	93	106	100
	EY-5	90	148	141	148	143	136	132	148	147
Çitgöl-Naşa	ÇİTGÖL-2	70	113	112	113	112	100	100	113	109
	NAŞA-1	51	93	95	93	94	79	80	94	87
Eynal	EY-Ç	78	111	110	111	110	97	97	111	106
	EY-G	68	113	112	113	112	100	100	113	109
	EY-E	66	117	115	117	116	104	103	117	113
Çitgöl-Naşa	EY-K	68	92	94	92	93	78	79	92	86
	NŞ-Ç	52	85	88	85	86	70	72	85	78
	NŞ-N	43	104	104	104	104	90	91	104	98
Eynal	EJ-1 <sup>+</sup>	162 <sup>*</sup>	145	139	145	141	134	129	145	144
	E-7 <sup>+</sup>	52	191	177	192	179	184	171	192	195
	E-8 <sup>+</sup>	161 <sup>*</sup>	167	158	168	160	158	149	167	168
	EJ-3 <sup>+</sup>	151 <sup>*</sup>	167	158	168	160	158	149	167	168

<sup>a</sup>Fournier (1977); <sup>b</sup>Fournier and Potter (1982); <sup>c</sup>Amorsson (2000); <sup>d</sup>Verma and Santoyo (1997); <sup>e</sup>Verma (2000); \*Well, \*Bottom-hole temperature.

Fournier's (1977) quartz (85–191 °C), Fournier and Potter's (1982) quartz (85–192 °C), Verma and Santoyo (1997) quartz (85–192 °C) and Verma (2000) quartz (78–195 °C) geothermometers reported a temperature range of 78–195 °C, indicating a reservoir temperature approximately 10 °C higher than the aforementioned temperature range.

### Cation geothermometers

For almost all of the water samples, the reservoir temperatures calculated using cation geothermometers (except for Na-Li and K-Mg geothermometers) were higher than temperatures calculated with silica geothermometers (Table 5). This is because silica geothermometers indicate the supply water temperature for the reservoir while the Na-K geothermometers in particular indicate deeper and hotter systems (see also Verma *et al.*, in press).

Of the Na-K geothermometers, the highest temperatures (221–249 °C) were predicted by the geothermometer developed by Giggenbach (1988). Arnorsson's (1983), Fournier's (1979), Can's (2002) and Verma and Santoyo's (1997) Na-K geothermometers indicate temperature ranges (181–237 °C) that are similar to each other but higher than other geothermometers.

Temperatures calculated with the Na-Li geothermometer developed by Kharaka and Mariner (1989) indicated a reservoir temperature of 173–174 °C, which was similar to the quartz geothermometer results for Eynal area water samples. On the other hand, Na-Li geothermometer by Verma and Santoyo (1997) pointed out to bottom hole temperatures of 114–116 °C. Temperatures calculated with Giggenbach's (1988) K-Mg geothermometer, which reflects temperatures at shallow depths before the geothermal fluid reaches the surface, indicated a reservoir temperature range of 141–178 °C. Na-K geothermometers indicate higher temperatures than expected for geothermal fluids that have a high concentration of calcium (Ca). Since

water in Eynal has a relatively low calcium content, the Na-K-Ca geothermometer developed by Fournier and Truesdell (1973) was applied for those samples. Reservoir temperatures in the range of 193–234 °C were estimated for those water samples, which are in harmony with the temperatures obtained by other Na-K geothermometers.

### Na-K-Mg diagram

Figure 3 presents an evaluation of all of the Simav thermal water samples in a Na–K–Mg diagram developed by Giggenbach (1988). Caution is however required to use ternary diagrams (Butler, 1979; Philip *et al.*, 1987). It is evident from the diagram that none of the Simav thermal water samples shows fluid-rock equilibrium and that the water is probably not fully equilibrated. It can be said that most of the water samples in the diagram fall in the region of immature water and on the border that separates the partially equilibrated water region from the immature water region. Aside from these samples, most of the spring water samples taken from the Eynal area in 1983 and 1984 fall in the region of partially equilibrated water. From this, it is possible to conclude that when compared with water in the Çitgöl-Naşa area, water in the Eynal area is more mature, less affected by processes caused by underground water (such as mixing, dilution, etc.) and is characterized as water that is closer to the conditions in the reservoir. In addition, because these samples fall in the region of partially equilibrated water or equilibrated and mature water, the application of the cation geothermometers on the samples will give somewhat reliable results. For this reason, the cation geothermometer temperatures for the water samples that fell in the region of partially equilibrated water were calculated (Table 5). On the other hand, the linear trend formed by all of the water samples on the diagram might indicate a reservoir temperature that is equilibrated at approximately 230–240 °C. This temperature is within the reservoir temperature

Table 5. Discharge temperature and temperatures (°C) obtained for Simav thermal waters with cation geothermometers.

Region	Sample	T (°C)	Na-K <sup>a</sup>	Na-K <sup>b</sup>	Na-K <sup>c</sup>	Na-K <sup>d</sup>	Na-K <sup>e</sup>	Na-K <sup>f</sup>	Na-K <sup>g</sup>	K-Mg <sup>d</sup>	Na-Li <sup>h</sup>	Na-Li <sup>c</sup>	Na-K-Ca <sup>a</sup>
	Ey	60	196	225	205	240	228	210	214	141	173	114	220
	Ey-2	74	209	235	217	249	237	220	223	152	-	-	231
	Ey-3	63	209	235	217	249	237	221	224	149	174	116	234
	Ey-4	96	186	218	197	234	221	203	207	150	174	116	230
	Ey-6	60	196	225	205	240	228	210	214	141	173	114	220
Eynal	SE-1	86	167	205	181	221	208	189	193	162	-	-	193
	SE-16	68	173	209	185	225	212	193	197	164	-	-	214
	SE-36	64	193	223	202	238	226	208	211	154	-	-	203
	SE-43	52	184	217	195	232	220	202	205	178	-	-	206
	SE-47	70	176	211	188	227	214	196	200	158	-	-	197
	SE-48	62	187	219	197	234	222	204	207	167	-	-	213

<sup>a</sup>Fournier and Truesdell (1973); <sup>b</sup>Fournier (1979); <sup>c</sup>Arnorsson (1983); <sup>d</sup>Giggenbach (1988); <sup>e</sup>Verma and Santoyo (1997); <sup>f</sup>Arnorsson (2000); <sup>g</sup>Can (2002); <sup>h</sup>Kharaka and Mariner (1989).

range (205–249 °C) recommended by Verma and Santoyo (1997), Fournier’s (1979) and Giggenbach’s (1988) Na-K geothermometers.

**K-Mg-Ca geoinicator diagram**

If we assume that the geothermal fluid is equilibrated with calcite (CaCO<sub>3</sub>), it is possible to evaluate the partial pressure for CO<sub>2</sub> (P<sub>CO<sub>2</sub></sub>) on the K-Mg-Ca geoinicator diagram (Figure 4). In the diagram developed by Giggenbach (1988), almost all of the thermal water samples are under the line of full equilibrium and are located in the region of water that has not matured with the formation of calcite. In addition, most water samples tend to fall between the line for granitic rock dissolution and the line for average crust rock dissolution. From this diagram, it is evident that water was formed as a result of rock dissolving into thermal water. This diagram shows that the water composition at final equilibrium temperatures (t<sub>km</sub>) is limited by calcite precipitation due to CO<sub>2</sub>.

**Na-K-Mg-Ca diagram**

Another evaluation of temperature and fluid-rock equilibrium based on cation ratios can be performed with the Na-K-Mg-Ca diagram recommended by Giggenbach

(1988). Figure 5 shows a diagram that evaluates 10Mg<sup>2+</sup>/(10Mg<sup>2+</sup>+Ca<sup>2+</sup>) versus 10K<sup>+</sup>/(10K<sup>+</sup>+Na<sup>+</sup>) for all of the Simav thermal water samples.

As is the case with the models in Figures 3 and 4, this model also does not indicate that the water samples have reached equilibrium between water and rock. However, if we investigate this diagram carefully, it is evident that the water samples from the Eynal area are closest to the complete equilibrium line for fluid-rock equilibrium, which is consistent with the model in Figure 3. Another conclusion drawn from the diagram is that most of the thermal water in the Simav region has become saline due to simple rock leaching or mixing with other water. In addition, by looking at the diagram it is easy to understand that the change in the ratio [10K<sup>+</sup>/(10K<sup>+</sup>+Na<sup>+</sup>)] (0.4-0.6) is significantly less than the change in the ratio [10Mg<sup>2+</sup>/(10Mg<sup>2+</sup>+Ca<sup>2+</sup>)] (0.1-0.9). This situation indicates that the K/Na ratio in the water is not strongly affected by the processes of dissolution and precipitation in the system. On the other hand, the fact that the Mg/Ca ratio is spread out over a large area indicates that the minerals that contain Ca and Mg (most likely carbonate minerals) are significantly affected by the dissolution and precipitation processes in the system.

Although the composition of the water samples do not indicate equilibrium between fluid and rock, it is evident that when the progressive trend of the group of water samples in the center of the diagram (which includes most of the water samples) is extended to the full equilibrium

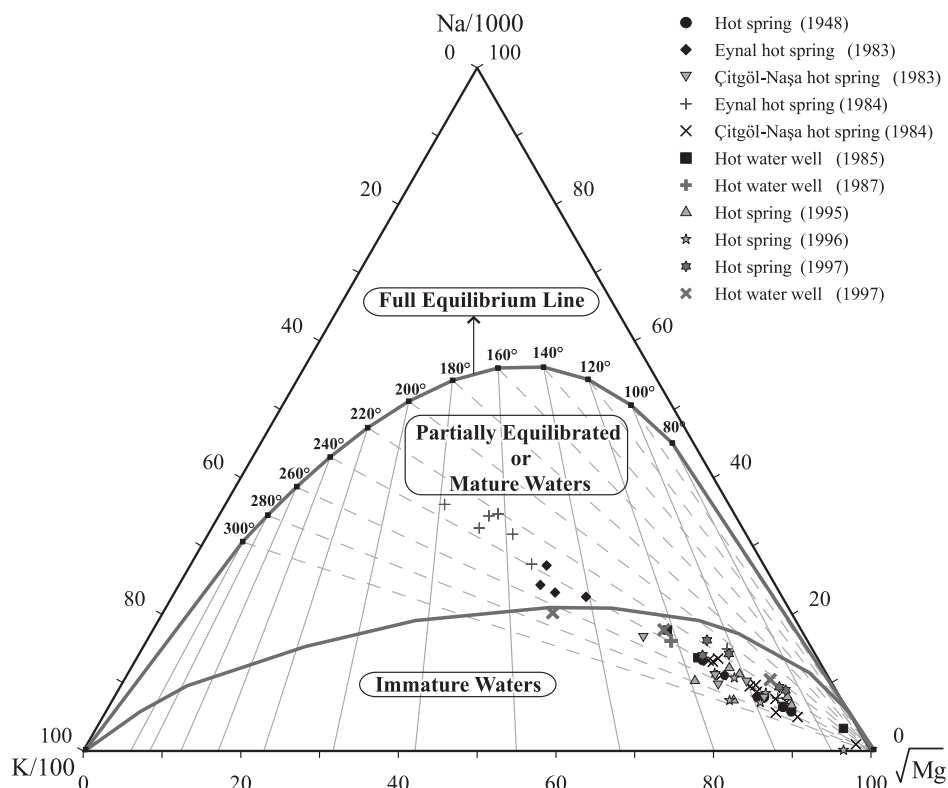


Figure 3. Na–K–Mg (mg/kg) diagram (Giggenbach, 1988) for samples of the Simav geothermal field.

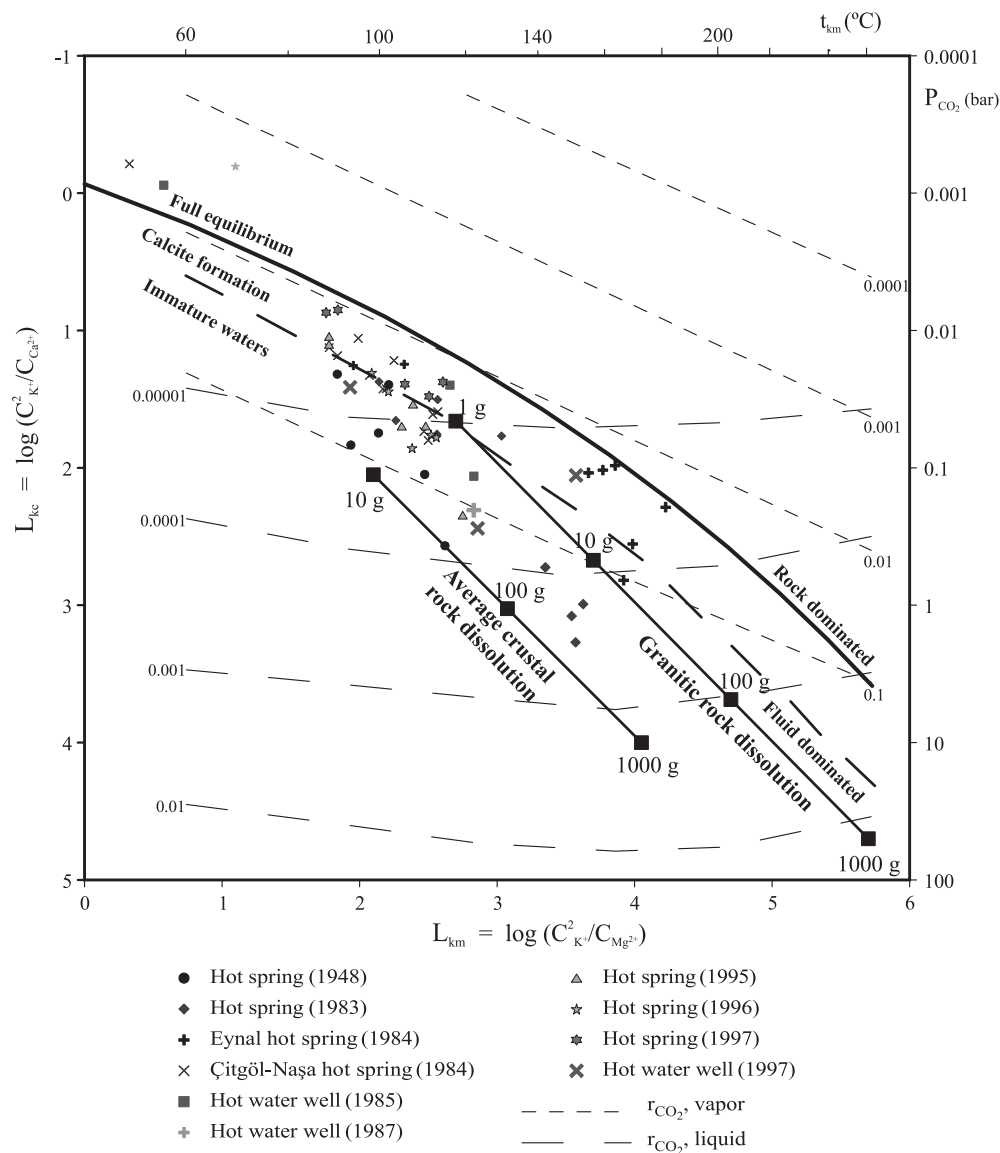


Figure 4. K–Mg–Ca geothermometer diagram for the evaluation of Na-K and K-Mg equilibration temperatures and of CO<sub>2</sub> fugacities by using K, Mg and Ca concentrations (Giggenbach, 1988) of Simav thermal waters.  $r_{CO_2}$ , mole ratio  $nCO_2/nH_2O$ ;  $t_{km}$ : K-Mg geothermometer temperature.

curve, a reservoir temperature consistent with the model in Figure 3 (230–240 °C) is indicated, pointing also to a deeper equilibrated source with a temperature of approximately 240 °C, which is hotter than the reservoir from which production is currently being carried out (approximately 160 °C).

### ISOTOPE CHEMISTRY

The isotope chemistry of a geothermal system provides information about the origin, dating and residence time of the geothermal fluid, the physical processes to which the water is subjected, the fluid-rock interaction and the reservoir.

### Origin and recharge of Simav thermal waters

Figure 6a shows the  $\delta^2H$ - $\delta^{18}O$  relationship for Simav water. From the diagram it is evident that the isotopic components of hot water samples fall below the line of local meteoric water (Imbach, 1997). The cold water sample from Nadarçam, however, falls near the line of local meteoric water. In addition, when compared with the wells (E-1 and E-7) and spring in the Eynal area, it is evident that the Naşa-2 spring in the Çitgöl-Naşa area has undergone more dilution with shallow water. As can be recalled from the previous models, water in the Çitgöl-Naşa area was more affected by dilution than water in the Eynal area. Figure 6a shows that Simav geothermal water

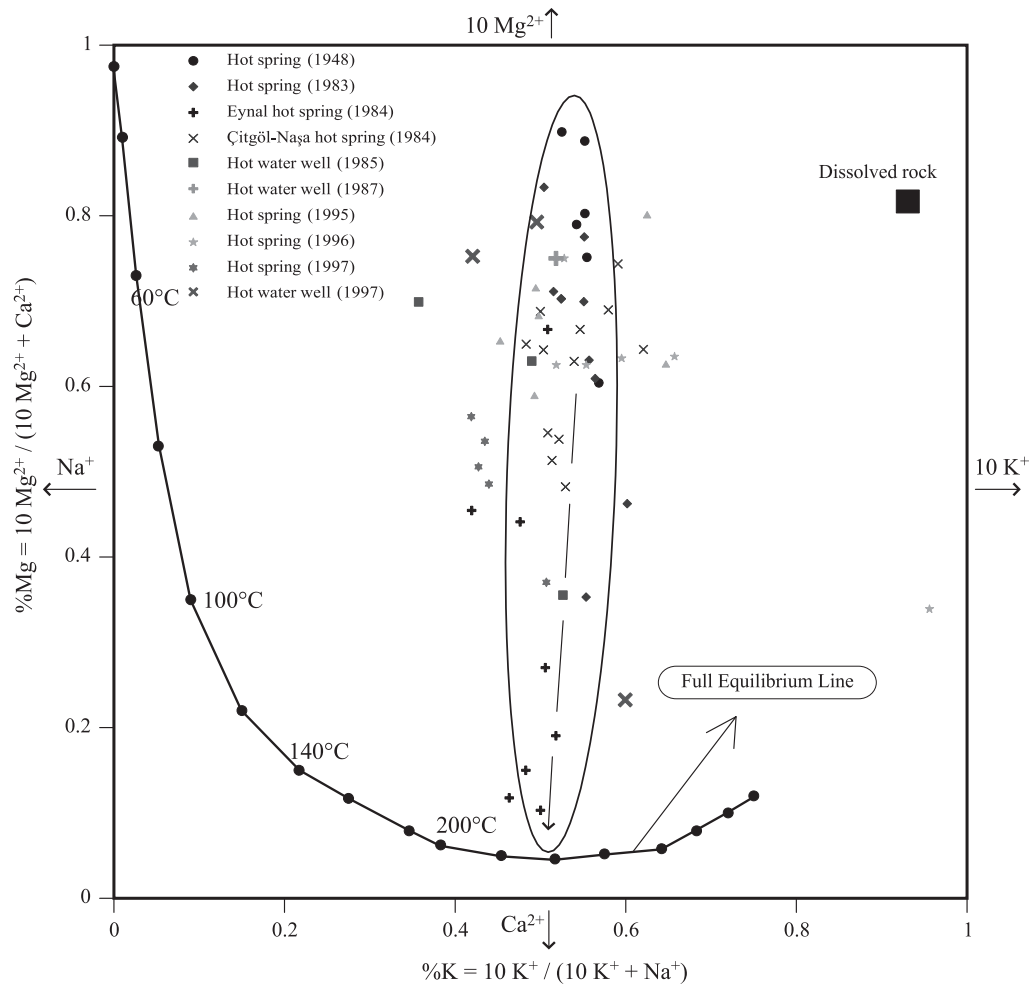


Figure 5. Na-K-Mg-Ca diagram for the evaluation of the attainment of full equilibrium with average crustal rock (Giggenbach, 1988) by using K, Mg and Ca concentrations of Simav thermal waters.

is enriched in  $^{18}\text{O}$ . This situation points to the existence of fluid-rock interaction in the system and/or boiling due to the high temperature in the reservoir. Also, the change of  $\delta^2\text{H}$  content in the water may indicate that the system is fed by water from a high altitude and/or comes from a long distance away.

Because the amount of tritium in meteoric water is higher than that in geothermal water, the increase in tritium at geothermal surface manifestations indicates that the system is being fed by meteoric water. In this regard,  $^3\text{H}$  (tritium)-Cl diagrams can be used to identify the direction of recharge and the mixture between geothermal water and underground water. Figure 6b shows the  $^3\text{H}$ -Cl relationship for Simav water. Based on the diagram in Figure 6b and tritium and chloride data (Table 6), the cold water sample from Nardaçam has the highest  $^3\text{H}$  (10.57 TU) and the lowest Cl (8.9 ppm) content. A line drawn from the Nardaçam cold water to the geothermal well and hot spring indicates the mixing line for the Simav field. As a result, it can be said that the thermal water is being fed by meteoric water in the Nardaçam area.

### Age of Simav thermal waters

Tritium ( $^3\text{H}$ ) is the isotope that is most widely used to identify the age and residence time of geothermal water. Table 6 shows the tritium data and the calculated ages for thermal water of Simav. From Table 6, it is apparent that the age of the water varies between about 35.7 and 60.6 years old. If we note that water containing 1-3 TU of tritium is considered to be 40-50 years old and that the tritium content of Simav geothermal water is between 0.36 and 1.44 TU, and if the error in the tritium measurement is taken into consideration, it can be said that Simav geothermal water is over 50 years old. However, it must not be forgotten that if geothermal water mixes with surface waters, this can cause errors in these age estimations.

### FLUID-MINERAL EQUILIBRIA

An evaluation of the chemical equilibrium between fluid and rock in geothermal systems requires information

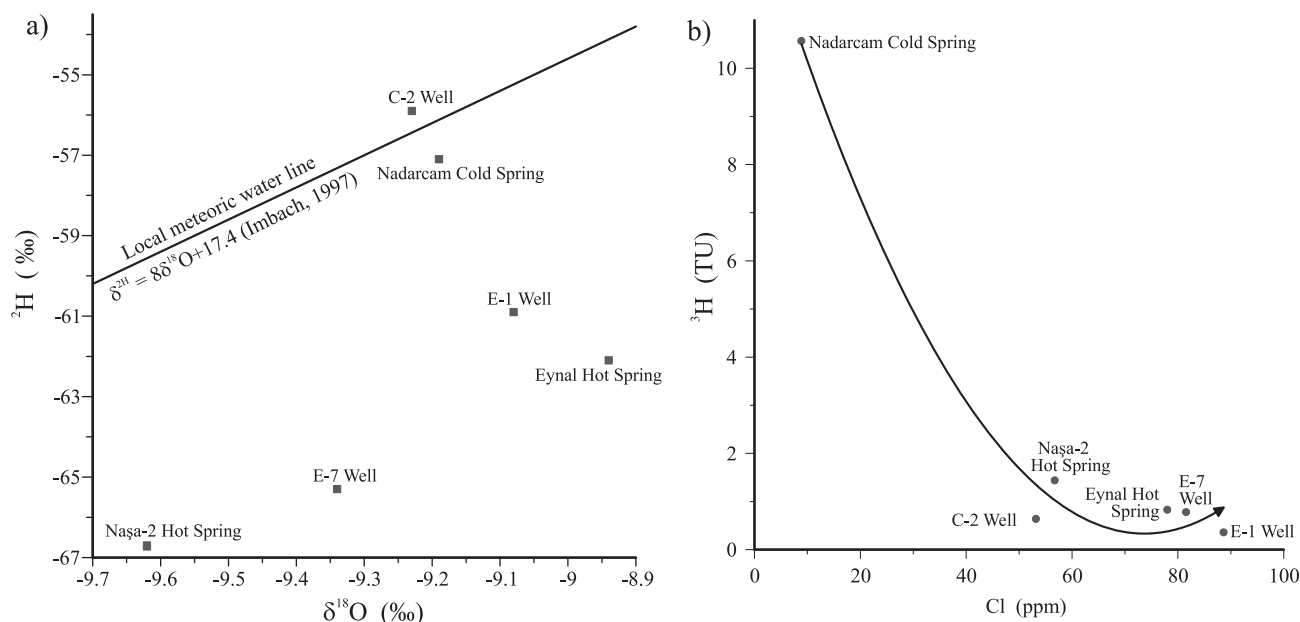


Figure 6. a: Isotopic evaluation of Simav waters using Deuterium-Oxygen-18 isotopes. b: Isotopic evaluation of Simav waters using Tritium-Chloride contents.

about the solubility of minerals in rocks that have undergone hydrothermal alteration and about the activity of the mineral types in the solution. Because of the large number of ions, ion pairs and complexes in the solution, generating the activity values for each type using existing analytic data (particularly at increasing temperatures) requires the use of a computer program. In this study, we made use of WATEQ4F (Ball and Nordstrom, 1991) and SOLVEQ (Reed and Spycher, 1990). Another computer program, SUPCRT-92 (Johnson *et al.*, 1992), was used to generate activity diagrams for minerals.

### Activity diagrams

Activity diagrams were used to investigate the fluid-mineral equilibrium of the Simav geothermal system. Diagrams were plotted for reservoir temperatures between 150 °C and 250 °C based on bottom-hole temperature data and temperatures estimated with silica and cation geothermometers (Figures 7a-d).

The generated activity diagrams show that as tempera-

ture increases, the stability fields of albite (Figure 7c), epidote (Figure 7b), Mg-chlorite (Figure 7d), gibbsite (Figure 7a), and muscovite (Figure 7a, c, d) increase. This indicates that these minerals are more stable at higher temperatures. On the other hand, the stability of K-feldspar at increasing temperatures is limited by the higher activity of K and the lower activity of Na, Mg and Ca. In addition, at higher temperatures, muscovite has the broadest activity range for K, but has the lowest activity for Mg and Ca. From Figure 7c, it can be seen that paragonite (Na-montmorillonite) is stable at temperatures of 150 °C and above.

When we inspect each of the activity diagrams, it is apparent that almost all of the thermal water (except for Figure 7d) is in equilibrium with K-feldspar, which is congruent with the findings from the other models. In Figure 7d, however, it is apparent that the water is in equilibrium with Mg-chlorite. When the temperature rises over 175 °C, Figure 7c indicates that the water is in equilibrium with K-feldspar, albite and muscovite; Figure 7b indicates that the water equilibrated with K-feldspar at 150 °C and equilibrated with zoisite (epidote) at temperatures of 175 °C and above; while Figure 7a indicates that the water

Table 6. Isotopic data and age estimations for Simav waters.

<sup>a</sup> Sample	Sampling date	δ <sup>18</sup> O (‰)	δ <sup>2</sup> H (‰)	<sup>3</sup> H (TU)	<sup>3</sup> H 2σ error	Cl (ppm)	t (year)
E-7 Well (51 °C <sup>b</sup> )	26.08.1997	-9.34	-65.3	0.78	0.28	81.5	46.7
Eynal Hot Spring (96 °C <sup>b</sup> )	26.08.1997	-8.94	-62.1	0.83	0.28	78	45.6
E-1 Well (142 °C <sup>c</sup> )	26.08.1997	-9.08	-60.9	0.36	0.27	88.6	60.6
ÇITGÖL-2 Well (105 °C <sup>c</sup> )	26.08.1997	-9.23	-55.9	0.64	0.28	53.2	50.3
Naşa-2 Hot Spring (50 °C <sup>c</sup> )	26.08.1997	-9.62	-66.7	1.44	0.28	56.7	35.7
Nadarçam Cold Spring (12 °C <sup>c</sup> )	26.08.1997	-9.19	-57.1	10.57	0.46	8.9	-

<sup>a</sup>Bayram and Simsek (2005); <sup>b</sup>off-spring temperature, <sup>c</sup>well temperature at depth of 65.8 m, <sup>d</sup>well temperature at depth of 46 m.

equilibrated with K-feldspar and muscovite. On the other hand, the fact that samples from spring Ey-2 and well EJ-1 are distinct from the other water samples and located in the upper portions of the diagrams is due to the high pH values (8.9 and 9.2) of these samples. In conclusion, since chlorite, albite, K-feldspar, epidote, muscovite and montmorillonite minerals were found in rock samples reported to be taken from the Simav environs, the activity diagrams concur with the field's alteration mineralogy and indicate that a potential source exists, which is a deeper and

hotter than the reservoir from which production is currently being carried out.

### Thermodynamic saturation states

Temperature-saturation index diagrams for minerals in the Simav thermal water (chalcedony, quartz, calcite, and muscovite) are shown in Figure 8a-d. The temperatures in the diagrams have been specified from the temperature

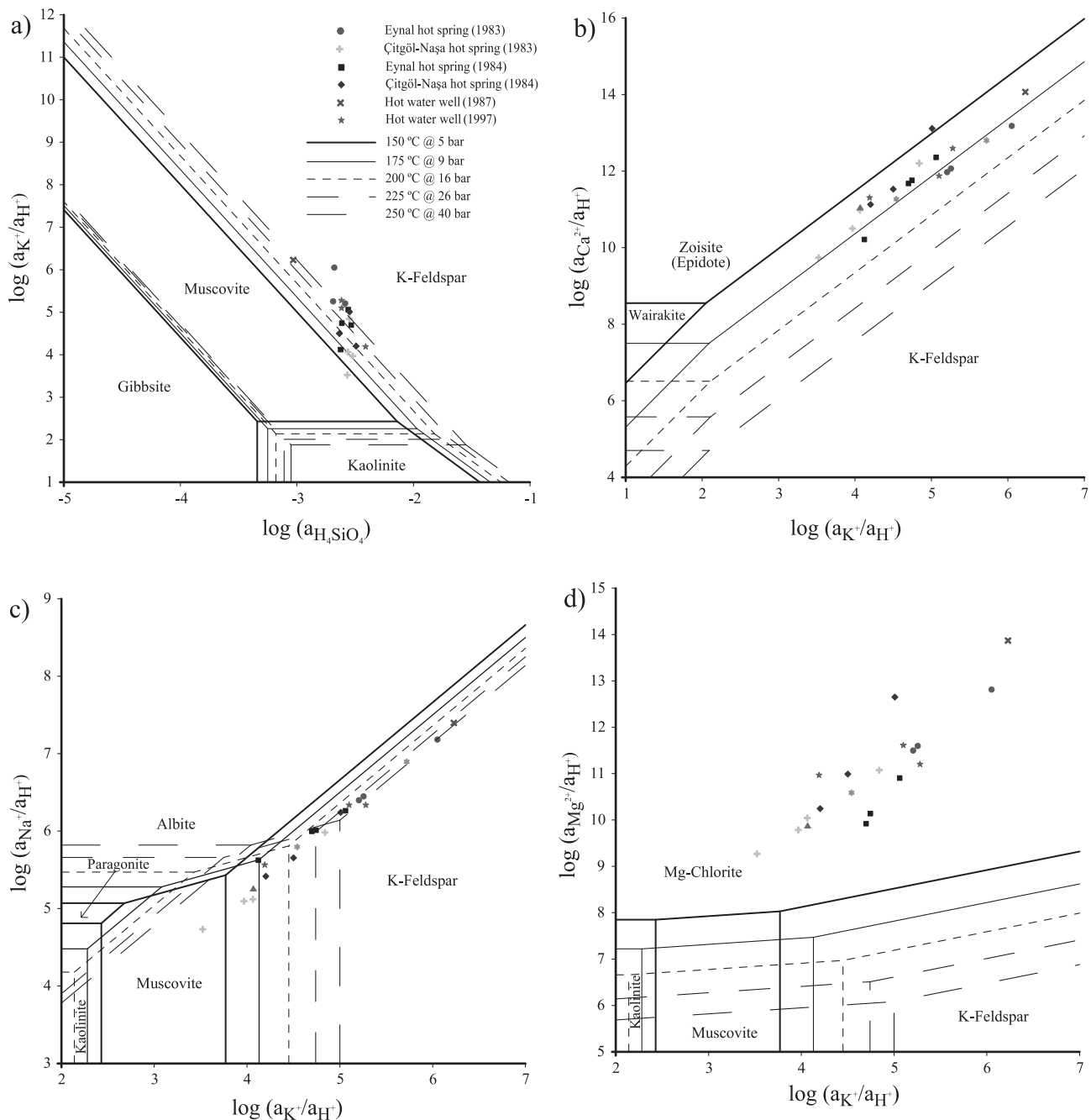


Figure 7. Activity diagrams for Simav thermal waters in the 150–250 °C temperature range for the systems (a)  $K_2O-SiO_2-Al_2O_3-H_2O$ , (b)  $CaO-K_2O-Al_2O_3-SiO_2-H_2O$ , (c)  $Na_2O-K_2O-Al_2O_3-SiO_2-H_2O$ , and (d)  $MgO-K_2O-Al_2O_3-SiO_2-H_2O$ .

at which each sample was measured (<100 °C) up to 250 °C in 25 °C increments such that they cover the temperature range calculated with chemical geothermometers and other models.

The diagram in Figure 8a was generated for chalcedony, a silica (SiO<sub>2</sub>) mineral, and indicates reservoir saturation temperatures of 125–150 °C. The diagram in Figure 8b was generated for quartz and indicates reservoir saturation temperatures of 150–175 °C, which correspond with the values obtained with the quartz geothermometers.

The slope of the curves indicates that precipitation occurs for chalcedony and quartz from low temperatures until the saturation temperature is reached, but after saturation has occurred, the minerals dissolve in the geothermal fluid from the equilibrium temperature to higher temperatures. Figure 8c was generated for calcite, which is a calcium carbonate mineral (CaCO<sub>3</sub>), and indicates that the water is oversaturated in calcite at all temperatures and that precipitation of calcite is probably occurring in the Simav geothermal field. Figure 8d, generated for muscovite, indicates reservoir

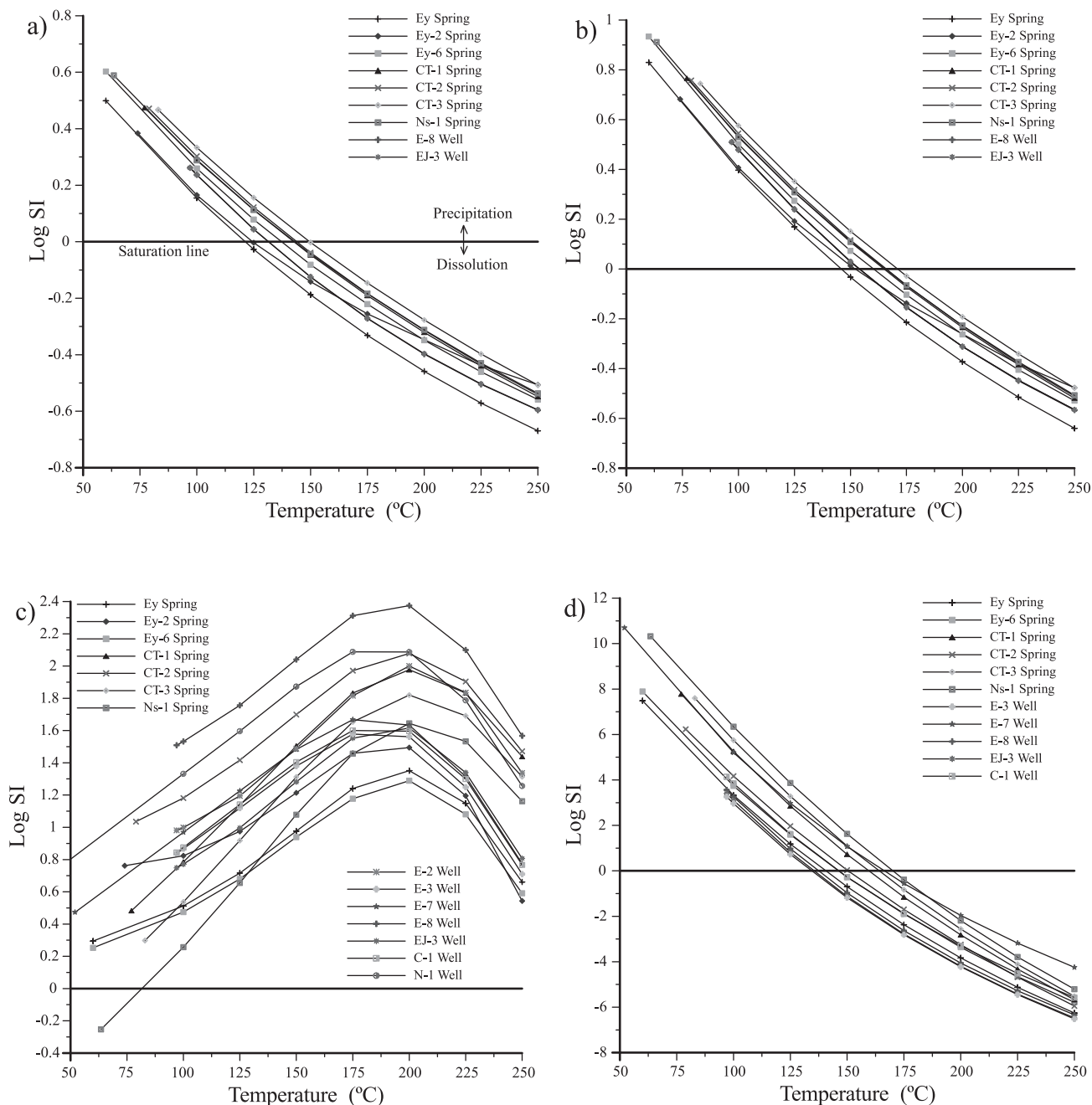


Figure 8. Mineral equilibrium diagrams for Simav thermal waters for (a) chalcedony (b) quartz, (c) calcite, and (d) muscovite.

saturation temperatures of 135–170 °C, which is congruent with values obtained with silica and K-Mg geothermometers. The figure also indicates that the solubility behavior of muscovite is similar to that of chalcedony and quartz. The same diagrams were also generated using the hot water spring data provided by Öktü (1984), resulting in similar conclusions.

## CONCLUSIONS

Thermal water in the Simav region can be classified as water that is affected by peripheral underground water that is rich in NaHCO<sub>3</sub>, contains high amounts of SO<sub>4</sub><sup>2-</sup> and low amounts of Cl<sup>-</sup>. Thermal waters in the Simav region are all related and have mixed close to the surface with underground water of meteoric origin. Thermal water from the Eynal area is less affected by dilution or mixing processes than water in the Çitgöl-Naşa area. Cation geothermometers applied to these samples will yield more reliable results than other samples.

Silica geothermometers indicate temperatures a little bit higher than the measured bottom hole temperatures (70–195 °C), and on the other hand, cation geothermometers and geothermometers give deep thermal water temperatures of 173–249 °C, which are consistent with the temperatures indicated by the field geological model and alteration mineralogy.

The delta deuterium ( $\delta^2\text{H}$ ) –delta oxygen-18 ( $\delta^{18}\text{O}$ ) diagram indicates <sup>18</sup>O enrichment for Simav geothermal water. This situation points to the existence of fluid-rock interaction in the system and/or boiling due to the high temperature in the reservoir. On the other hand, tritium (<sup>3</sup>H) – chloride (Cl) diagram shows that the Simav thermal water is partly fed by meteoric water from the Nadarçam area. The tritium content of the samples indicates that the age of Simav geothermal water is older than approximately 50 years.

The alteration mineralogy of rock samples collected the region indicates that chlorite, albite, K-feldspar, epidote, muscovite, illite and montmorillonite are probably in equilibrium with geothermal water and that the reservoir temperature could be between 160 °C and 250 °C. The activity diagrams concur with the field alteration mineralogy and the cation geothermometers, pointing to the existence of a source that is deeper and hotter than the reservoir from which production is currently being carried out.

Saturation index diagrams generated for Simav geothermal water using certain alteration minerals generally indicate reservoir temperatures that are similar to those given by silica geothermometers. On the other hand, chalcedony, quartz and muscovite precipitate from low temperatures until the equilibrium temperature is reached but dissolve in the geothermal fluid as the temperature increases. Calcite, however, is oversaturated at almost every temperature and precipitates.

## ACKNOWLEDGEMENTS

The authors would like to thank Ege Energy for providing data and would like to express special gratitude to the CEO, Muharrem Balat. Thanks are due especially to Dr. Halim Mutlu for his valuable help and to Tahir Öngür in particular for his valuable comments. We would like to extend our gratitude to Dr. Surendra P. Verma for his valuable efforts and help.

## REFERENCES

- Akdeniz, N., Konak, N., 1979, Geology of Simav-Emet-Tavsanlı-Dursunbey-Demirci regions [in Turkish]: Ankara, Mineral Research and Exploration of Turkey (MTA), 6547, 9-96.
- Akkus, I., Akilli, H., Ceyhan, S., Dilemre, A., Tekin, Z., 2005, Turkey's Geothermal Resource Inventory [in Turkish]: Ankara, Mineral Research and Exploration of Turkey (MTA), Inventory Series, 201, 521 p.
- Arnorsson, S., 1983, Chemical equilibria in Icelandic geothermal systems, Implications for chemical geothermometry investigations: *Geothermics*, 12, 119-128.
- Arnorsson, S., 2000, Isotopic and chemical techniques in geothermal exploration, development and use: Vienna, International Atomic Energy Agency, 156-187.
- Ball, J.W., Nordstrom, D.K., 1991, User's manual for WATEQ4F, with revised thermodynamic data base and test cases for calculating speciation of major, trace and redox elements in natural waters: United States Geological Survey (USGS), Open-File Report, 91-183.
- Barnett, V., Lewis, T., 1994, Outliers in statistical data: Chichester, John Wiley & Sons, 584 p.
- Bayram, A.F., Simsek, S., 2005, Hydrogeochemical and isotopic survey of Kütahya-Simav geothermal field, *in* World Geothermal Congress, Antalya, Turkey, 843, 3-5.
- Bevington, P.R., Robinson, D.K., 2003, Data reduction and error analysis for the physical sciences: Boston, McGraw Hill, 320 p.
- Bird, D.K., Schiffman, P., Elders, W.A., Williams, A.E., McDowell, S.D., 1984, Calc-silicate mineralization in active geothermal systems: *Economic Geology*, 79, 671-695.
- Browne, P.R.L., 1996, Hydrothermal Alteration: Auckland, University of Auckland, Geothermal Institute, Lecture Notes, 665.611, 32 p.
- Burcak, M., Sevim, F., Hacisalihoglu, O., 2007, Discovering a new buried geothermal field which have been found out using geological-geophysical and geochemical methods in Uchbash-Shaphane, Kutahya western Anatolia, Turkey, *in* Thirty-Second Workshop on Geothermal Reservoir Engineering, Proceedings, Stanford: California, Stanford University, SGP-TR-183, 2-3.
- Butler, J.C., 1979, Trends in ternary petrologic variation diagrams - fact or fantasy?: *American Mineralogist*, 64, 1115-1121.
- Can, I., 2002, A new improved Na/K geothermometers by artificial neural networks: *Geothermics*, 31, 751-760.
- Cemen, I., Seyitoglu, G., Isik, V., 2002, Extensional tectonics in southern Basins and Ranges, United States, and in western Turkey: A review of similarities, differences and problems, *in* Geological Society of America Annual Meeting, Denver Colorado, USA, Paper 79-1.
- Caglar, K.Ö., 1948, Turkey's mineral waters and hot springs [in Turkish]: Ankara, Mineral Research and Exploration of Turkey (MTA) Publications, 11, 461-468.
- Erisen, B., Can, A.R., Yildirim, N., 1989, EJ-I and EJ-II geothermal wells completion reports of Simav-Eynal (Kütahya) geothermal region [in Turkish]: Ankara, Mineral Research and Exploration of Turkey (MTA), 8916, 60 p.
- Fara, M., Chandrasekharam, D., Minissale, A., 1999, Hydrogeochemistry of Damt thermal springs, Yemen Republic: *Geothermics*, 28,

- 241-252.
- Fournier, R.O., 1977, Chemical geothermometers and mixing models for geothermal systems: *Geothermics*, 5, 41-50.
- Fournier, R.O., 1979, A revised equation for the Na/K geothermometer: *Geothermal Resources Council (GRC) Transactions*, 3, 221-224.
- Fournier, R.O., Potter, R.W., 1982, A revised and expanded silica (quartz) geothermometer: *Geothermal Resources Council (GRC) Bulletin*, 11(10), 3-12.
- Fournier, R.O., Truesdell, A.H., 1973, An empirical Na-K-Ca geothermometer for geothermal waters: *Geochimica et Cosmochimica Acta*, 37, 1255-1275.
- Giggenbach, W.F., 1988, Geothermal solute equilibria. Derivation of Na-K-Ca-Mg geoindicators: *Geochimica et Cosmochimica Acta*, 52, 2749-2765.
- Güven, M., Taskin, I., 1985, Simav-Naşa (Kütahya) hot water well (N-1) completion report [in Turkish]: Ankara, Mineral Research and Exploration of Turkey (MTA), 7903, 12 p.
- Hochstein, M.P., 1990, Geothermal resources: classification and assessment of geothermal resources: Pisa, Italy, International Institute for Geothermal Research, International School of Geothermics, 2, 31-57.
- Hochstein, M.P., Zhongke, Y., Ehara, S., 1990, The Fuzhou geothermal system (People's Republic of China): Modelling study of a low temperature fracture-zone system: *Geothermics*, 19(1), 43-60.
- Ilkisik, M., 1995, Regional heat flow in Western Anatolia using silica temperature estimates from thermal springs: *Tectonophysics*, 244, 175-184.
- Imbach, T., 1997, Geology of Mount Uludağ with emphasis on the genesis of the bursa thermal waters, northwest Anatolia, Turkey. Active tectonics of northwestern Anatolia, in Schindler, C., Pfister, M., Aksoy, A., Marmara Poly-Project (eds.), *The Marmara Poly-Project: a Multidisciplinary Approach by Space-geodesy, Geology, Hydrogeology, Geothermics and Seismology*: Zürich, vdf Hochschulverlag AG an der ETH, 253 p.
- Johnson, J.W., Oelkers, E.H., Helgeson, H.C., 1992, A software package for calculating the standard molal thermodynamic properties of mineral, gases, aqueous species, and reactions from 1 to 5000 bar and 0 to 1000 °C: *Computers and Geosciences* 18(7), 899-947.
- Kassoy, D.R., Zebib, A., 1978, Convection fluid dynamics in a model of a fault zone in the earth crust: *Journal of Fluid Mechanics*, 88, 769-792.
- Kharaka, Y.K., Mariner, R.H., 1989, Chemical geothermometers and their application to formation waters from sedimentary basins, in Naeser, N.D., McCulloh, T.H., (eds.), *Thermal History of Sedimentary Basins: Methods and Case Histories*: New York, Springer-Verlag, 99-117.
- Mutlu, H., Gulec, N., 1998, Hydrogeochemical outline of thermal waters and geothermometry applications in Anatolia (Turkey): *Journal of Volcanology and Geothermal Research*, 85, 495-515.
- Oygür, V., Erler, A., 2000, Metalogeny of Simav graben [in Turkish]: *Geological Bulletin of Turkey*, 43(1), 7-19.
- Öktü, G., 1984, Hydrological investigation of Eynal and Çitgöl-Naşa (Simav) hot springs [in Turkish]: Ankara, Mineral Research and Exploration of Turkey (MTA), 7737, 15-44.
- Öngür, T., 2004, Capacity of Simav geothermal region. Geological Evaluation [in Turkish]: Ege Enerji Company, Report, 3 p.
- Philip, G.M., Skilbeck, C.G., Watson, D.F., 1987, Algebraic dispersion fields on ternary diagrams: *Mathematical Geology*, 19, 171-181.
- Reed, M.H., Spycher, N.F., 1990, User's guide for SOLVEQ: A computer program for computing aqueous-mineral-gas equilibria: Eugene: Oregon, University of Oregon, Department of Geological Sciences, 4-37.
- Ring, U., Johnson, C., Hetzel, R., Gessner, K., 2003, Tectonic denudation of a Late Cretaceous-Tertiary collisional belt: Regionally symmetric cooling patterns and their relation to extensional faults in Anatolide belt of western Turkey: *Geological Magazine*, 140(4), 421-441.
- Serpen, U., Mihcakan, M., 1999, Heat flow and related geothermal potential of Turkey, in *Geothermal Resources Council (GRC) Annual Meeting*, GRC Transactions, 23, 485-490.
- Verma, M.P., 2000, Revised quartz solubility temperature dependence equation along the water-vapor saturation curve, in *World Geothermal Congress, Kyushu-Tohoku, Japan, 1927-1932*.
- Verma, S.P., Santoyo, E., 1997, New improved equations for Na/K, Na/Li and SiO<sub>2</sub> Geothermometers by outlier detection and rejection: *Journal of Volcanology and Geothermal Research*, 79, 9-23.
- Verma, S.P., Quiroz-Ruiz, A., 2006a, Critical values for six Dixon tests for outliers in normal samples up to sizes 100, and applications in science and engineering: *Revista Mexicana de Ciencias Geológicas*, 23(2), 133-161.
- Verma, S.P., Quiroz-Ruiz, A., 2006b, Critical values for 22 discordancy test variants for outliers in normal samples up to sizes 100, and applications in science and engineering: *Revista Mexicana de Ciencias Geológicas*, 23(3), 302-319.
- Verma, S.P., Díaz-González, L., Sánchez-Upton, P., Santoyo, E., 2006, OYNLY: A new computer program for ordinary, York, and New York least-squares linear regressions: *World Scientific and Engineering Academy and Society (WSEAS), Transactions on Environment and Development*, 2(8), 997-1002.
- Verma, S.P., Pandarinath, K., Santoyo, E., in press, SolGeo: A new computer program for solute geothermometers and its application to Mexican geothermal fields: *Geothermics*.
- Yurtseven, D., Özgür, R., Uzel, Ö.F., 1998, Kütahya-Simav Eynal E-7, E-8 and EJ-3 Wells Completion Report (in Turkish): Ankara, Mineral Research and Exploration of Turkey (MTA), 18-57.
- Yücel, B., Coskun, B., Demirci, S., Yildirim, N., 1983, Geology and geothermal potential of Simav (Kütahya) Region [in Turkish]: Ankara, Mineral Research and Exploration of Turkey (MTA), 8219, 27 p.
- Zhongke, Y., Shengbiao, H., Hochstein, M.P., 1990, Conceptual model of the Zhangzhou low temperature system and its surrounding catchment (Fujian Province, P.R. China), in *15<sup>th</sup> Workshop on Geothermal Reservoir Engineering, Proceedings, Stanford: California, Stanford University*, 97-102.

Manuscript received: April 11, 2008

Corrected manuscript received: June 4, 2008

Manuscript accepted: June 4, 2008